Available online at www.sciencedirect.com
ScienceDirect
Bioorganic & Medicinal Chemistry 16 (2008) 5962–5973
Bioorganic & Medicinal Chemistry

Inhibitory effects of a series of 7-substituted-indazoles toward nitric oxide synthases: Particular potency of 1*H*-indazole-7-carbonitrile

Betty Cottyn,[a] Francine Acher,[b] Booma Ramassamy,[b] Luke Alvey,[a] Michel Lepoivre,[c] Yves Frapart,[b] Dennis Stuehr,[d] Daniel Mansuy,[b] Jean-Luc Boucher[b] and Dominique Vichard[a,*]

[a]*Institut Lavoisier, CNRS UMR 8180, Université de Versailles, 45 Avenue des Etats Unis, 78035 Versailles cedex, France*
[b]*Laboratoire de Chimie et Biochimie Pharmacologiques et Toxicologiques, CNRS UMR 8601, Université Paris Descartes, 45 rue des Saints-Pères, 75270 Paris, France*
[c]*CNRS UMR 8619, IBBMC, Université Paris Sud-Orsay, Bat 430, 91105 Orsay, France*
[d]*Department of Immunology, Lerner Research Fundation, Cleveland Clinic, Cleveland, OH 44195, USA*

Received 25 January 2008; revised 15 April 2008; accepted 23 April 2008
Available online 26 April 2008

Abstract—A series of new 7-monosubstituted and 3,7-disubstituted indazoles have been prepared and evaluated as inhibitors of nitric oxide synthases (NOS). 1*H*-Indazole-7-carbonitrile (**6**) was found equipotent to 7-nitro-1*H*-indazole (**1**) and demonstrated preference for constitutive NOS over inducible NOS. By contrast, 1*H*-indazole-7-carboxamide (**8**) was slightly less potent but demonstrated a surprising selectivity for the neuronal NOS. Further substitution of **6** by a Br-atom at carbon-3 of the heterocycle enhanced 10-fold the inhibitory effects. Inhibition of NO formation by **6** appeared to be competitive versus both substrate and the cofactor (6*R*)-5,6,7,8-tetrahydro-L-biopterin (H_4B). In close analogies with **1**, compound **6** strongly inhibited the NADPH oxidase activity of nNOS and induced a spin state transition of the heme–Fe^{III}. Our results are explained with the help of the X-ray structures that identified key-features for binding of **1** at the active site of NOS.

1. Introduction

Nitric oxide (NO) is an endogenously produced free radical, which has important biological functions in mammals.[1–3] NO acts as a second messenger molecule through the activation of its main target, soluble guanylate cyclase. In the cardiovascular system, it is implicated in the regulation of vascular tone, platelet aggregation, and leukocyte adhesion on the endothelial surface. In the central nervous system and in the peripheral non-adrenergic non-cholinergic nerves, NO is a potent neurotransmitter involved in long-term potentiation, migraine, and gastric motility. Elsewhere, NO is a cytotoxic and cytostatic agent associated with phagocytic cells in the immune system.[1–3]

NO is synthesized by oxidation of the amino acid L-arginine (L-arg) catalyzed by three distinct isoforms of heme proteins called NO synthases (NOS).[4–6] The neuronal (nNOS) and endothelial NOS (eNOS) are constitutively expressed and are Ca^{++}- and calmodulin (CaM)-dependent enzymes, whereas inducible NOS (iNOS) is expressed in response to an immune challenge.[4–6] All three isoforms contain an N-terminal domain (oxygenase domain) with binding sites for substrate, heme (Fe^{III}-protoporphyrin IX), and cofactor (6*R*)-5,6,7,8-tetrahydrobiopterin (H_4B), and a linked C-terminal domain (reductase domain) containing NADPH, FAD,

Abbreviations: L-arg, L-arginine; CaM, calmodulin; DTT, dithiothreitol; H_4B, (6*R*)-5,6,7,8-tetrahydro-L-biopterin; Hepes, *N*-(2-hydroxyethyl)piperazine-*N*′-2-ethane sulfonic acid; HS, high spin; ImH, imidazole; LS, low spin; NOS, nitric oxide synthase; n-, i- and eNOS, neuronal, inducible and endothelial NOS, respectively; $nNOS_{oxy}$, oxygenase domain of neuronal NOS; NO_2-arg, N^{ω}-nitro-L-arginine; SOD, superoxide dismutase.

Keywords: 7-Nitroindazole; Substituted indazoles; Nitric oxide synthase; Inhibitors.

* Corresponding author. Tel.: +33 1 39 25 44 71; fax: +33 1 39 25 44 52; e-mail: vichard@chimie.uvsq.fr

0968-0896/$ - see front matter © 2008 Elsevier Ltd. All rights reserved.
doi:10.1016/j.bmc.2008.04.056

FMN, and CaM binding sites.[4–6] The observed biological activities of NO are closely linked to the NOS isoform involved in its synthesis and overproduction of NO leads to toxic effects.[1–3] Overproduction of NO by iNOS results in severe deleterious effects in septic shock and tissue degradation during chronic inflammation while overproduction of NO by nNOS appears to be involved in neurodegenerative disorders. Therefore, selective NOS inhibitors would be interesting therapeutic agents for the treatment of the above-mentioned diseases. However, to have therapeutic value, NOS inhibitors must be selective of one of the three isoforms. In particular, iNOS and nNOS inhibitors must not interfere with eNOS that plays key roles in vasodilation and blood pressure regulation.[1–3]

Several classes of reversible and irreversible NOS inhibitors have been described.[7–9] Substrate analogues such as N^{ω}-nitro-L-arginine (NO_2-arg), N^{ω}-methyl-L-arginine, thio-L-citrulline, NO_2-arg containing dipeptides, and heterocyclic compounds are widely used as NOS inhibitors in in vitro studies.[7–15] Even though highly in vitro isoform-selective inhibitors are now available, only a few compounds have shown to be selective toward nNOS in vivo. Moore and co-workers first reported the potent inhibitory effects of the heterocyclic compound 7-nitro-1*H*-indazole, **1**.[16,17] This compound exhibits a clear anti-nociceptive activity without altering blood pressure in vivo and is extensively used as a selective inhibitor of nNOS that evidences a 10-fold selectivity for nNOS over iNOS.[16–18] However, **1** inhibits nNOS by competing with both L-arg and H_4B and it is noteworthy that, despite its selectivity for nNOS in vivo, **1** inhibits the three NOS isoforms to a similar extent under in vitro conditions.[12,13]

Furthermore, potential future uses of **1** could be limited by its nitroaromatic nature. Actually, nitroaromatic compounds often lead to toxic effects in vivo that are linked either to their ability to start futile cycles of O_2 reduction leading to superoxide anion and related species, or to their metabolic reduction into reactive electrophilic metabolites such as aromatic hydroxylamines or nitroso compounds.[19] Thus, secondary toxic effects of nitrofurantoin or nitroimidazole drugs have been related to reactive metabolite formation upon reductive metabolism of the nitro-function of these drugs.[20]

In order to avoid such possible toxic effects of **1**, we have synthesized a series of new 7-substituted indazoles bearing an electron-withdrawing substituent, distinct from a nitro group. The choice of keeping an electron-withdrawing substituent on position 7 was made on the basis of previous studies that showed that substitution of the heterocycle by a NO_2 group at the 4-, 5-, or 6-position leads to less active compounds than at the 7-position.[12,16,18,21] Substitution of the indazole nucleus by the electron-donating methoxy group at the 4-, 5-, 6-, or 7-position leads to a decrease of the inhibitory activity but the 7-methoxy derivative remains the most potent isomer in this series.[22–24] The higher affinity of **1** for NOSs when compared to 7-methoxy-1*H*-indazole has been attributed to the existence of a stronger H-bond between one oxygen-atom of the nitro group of **1** and a residue of the binding site than between the O-atom of the methoxy group and the same residue.[25,26]

Introduction of a Br-atom at the 3-position of **1**, in 3-bromo-7-nitro-1*H*-indazole **12**, is known to strongly enhance its inhibitory effects.[18] This has encouraged us to synthesize some new 3-bromo-7-substituted indazole derivatives. In addition to the nitro group, it has been proposed that the *N*(1)-H group of **1** is also able to establish an hydrogen bond with a residue of the active site.[27,28] In order to get new information about the importance of this *N*(1)-H group, we have synthesized *N*(1)-methyl analogues of **1** and **12** that should disrupt this H-bond.

This series of indazole derivatives was evaluated as inhibitors of purified recombinant n-, i,- and eNOS. Two of them, 1*H*-indazole-7-carbonitrile **6**, and its 3-bromo derivative, 3-bromo-1*H*-indazole-7-carbonitrile **14**, were found to be potent inhibitors for nNOS and slightly more isoform-selective than **1** and its 3-bromo derivative **12**.

2. Chemistry

Our first target molecule was 1*H*-indazole-7-carbonitrile **6**. Moore and co-workers have suggested that this compound could be a NOS inhibitor but its synthesis had not been reported when we started this work.[17] In order to design a general and efficient approach that would allow an easy preparation of **6** and new 7-monosubstituted indazole derivatives, we first envisioned that they could be practically obtained via a palladium-mediated cyanation reaction from 1*H*-indazol-7-yl trifluoromethanesulfonate **3**. New triflate **3** was obtained in an almost quantitative yield by trifluoromethanesulfonation of 1*H*-indazol-7-ol **2** by *N*-(2-pyridyl)triflimide[29] in the presence of Cs_2CO_3 and K_2CO_3 without competitive *N*-triflation. However, triflate **3** failed to participate in the palladium-catalyzed cyanation and was recovered unchanged. We found an efficient alternative by preparing 7-iodo-1*H*-indazole **5** using a diazotization/iodination sequence starting from 1*H*-indazol-7-amine **4** (Scheme 1). Amine **4** was quantitatively obtained by

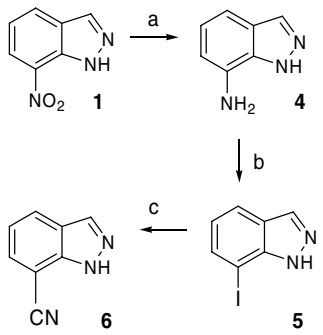

Scheme 1. Synthesis of 7-substituted indazoles **4**–**6**. Reagents and conditions: (a) Pd/C, HCO_2NH_4, EtOH, reflux; (b) $NaNO_2$, KI, HCl, 0 °C then rt; (c) dppf, $Pd_2(dba)_3$, Zn, $Zn(CN)_2$, DMAC, 120 °C.

reduction of **1** by ammonium formate in the presence of Pd/C.[30] Further diazotization of **4** and reaction with KI led to 7-iodo-1*H*-indazole **5** in 53 % overall yield from **1**. We were delighted to observe that our recently described methodology afforded **6** in a reproducible 63% yield from **5** with no need for protection of any nitrogen atom.[31] 1*H*-Indazole-7-carbonitrile **6** was a versatile precursor for compounds **7-9** and the 3-bromo-derivatives **14-16** (Scheme 2). Acidic hydrolysis of **6** quantitatively provided 1*H*-indazole-7-carboxylic acid **7**. Interestingly, only two syntheses of **7** have been recently patented. The first one is based on lithiation of 7-bromo-1*H*-indazole followed by addition of CO_2 while the second one involves the cyclization of 2-amino-3-methylbenzoic acid.[32,33] Using the mixed anhydride method, **7** was quantitatively converted to 1*H*-indazole-7-carboxamide **8**.[34] Finally, 7-(1*H*-tetrazol-5-yl)-1*H*-indazole **9**, which can be considered as a bioisoster of **7**, was obtained using a Huysgens cycloaddition between **6** and Me_3SiN_3 in the presence of $AlMe_3$.[35] We next moved to the synthesis of the 3-bromo derivatives **13–16**. 3-Bromo-7-iodo-1*H*-indazole **13** and 3-bromo-1*H*-indazole-7-carbonitrile **14** (Scheme 2) were easily obtained from **5** and **6**, respectively, after regioselective bromination by *N*-bromosuccinimide in the presence of KOH following a previously described method.[36] Acidic hydrolysis of **14** afforded 3-bromo-1*H*-indazole-7-carboxylic acid **15** in an almost quantitative yield whereas 3-bromo-1*H*-indazole-7-carboxamide **16** was easily obtained by activation as a mixed anhydride and reaction with ammonia as described above for **8**.

In order to extend the structure-activity relationship profile, we next focussed on the preparation of 7-(1*H*-1,2,3-triazol-5-yl)-1*H*-indazole **11**. This compound was obtained from **5** using a Sonogashira coupling with trimethylsilylacetylene in the presence of tetrakis(triphenylphosphine)palladium followed by deprotection of the terminal alkyne **10**. Cycloaddition of compound **10** with trimethylsilylazide afforded triazole **11** in 55 % overall yield from **5** (Scheme 3).[37,38]

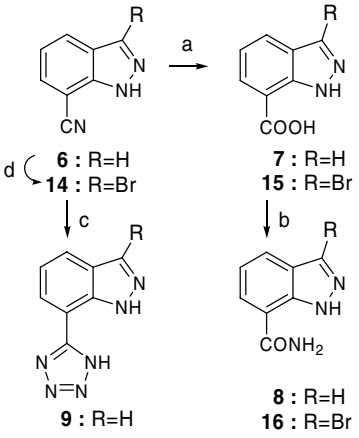

Scheme 2. Synthesis of 7-substituted indazoles **6–9** and 3-bromo derivatives **14–16**. Reagents and conditions: (a) 6 N HCl, reflux; (b) NEt_3, $ClCO_2Et$, CH_2Cl_2, −20 °C, then NH_3, −20 °C; (c) Me_3SiN_3, $AlMe_3$, toluene, 0 °C then 80 °C; (d) NBS, NaOH, DMF, rt.

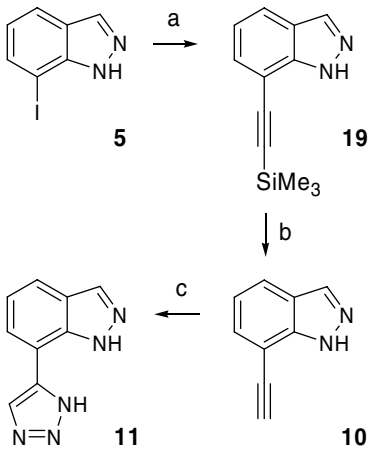

Scheme 3. Synthesis of triazole **11**. Reagents and conditions: (a) $Me_3Si–C{\equiv}CH$, $Pd(PPh_3)_4$, CuI, NEt_3, CH_3CN, rt; (b) K_2CO_3, MeOH, rt; (c) Me_3SiN_3, CuI, MeOH, DMF, 120 °C.

Selective methylation of the *N*(1)-H group of **1** and **12** was performed by treatment with CH_3I in the presence of KOH as previously described.[36] 1-Methyl-7-nitro-1*H*-indazole **17** and 3-bromo-1-methyl-7-nitro-1*H*-indazole **18** were obtained in almost quantitative yields without any formation of the *N*(2)-methyl isomers.[36]

3. Results and discussion

3.1. Effects of the indazole derivatives on NO formation catalyzed by n-, i-, and eNOS

Compounds **1–18** were tested for their inhibitory effects on the oxidation of L-arg to NO catalyzed by the three recombinant isoforms of NOS containing all their cofactors. The rates of NO formation by NOS were measured using the oxidation of oxyhemoglobin to methemoglobin by NO following a usual protocol.[39] For comparative purposes, **1** and **12**, two already known inhibitors of NOSs, were included in this study.[12,13,16–18] Under our conditions, **1** appeared to be a good but almost non-selective inhibitor of the three NOSs, with IC_{50} values of 25 ± 5, 50 ± 10, and 35 ± 5 μM towards n-, i-, and eNOS, respectively (Table 1). Compound **12** was also a non-selective inhibitor about 10-fold more potent than **1** with IC_{50} values around 2 μM, in agreement with previous literature data.[18] From this series of 7-substituted indazoles, compound **6** gave the best results with IC_{50} values similar to those observed with **1** towards nNOS and eNOS. Its selectivity for nNOS versus iNOS was two times better than that of **1** (determined at a simple ratio of the IC_{50} values). As previously observed with **1**, introduction of a 3-bromo substituent into compound **6** led to a strong increase of the inhibitory potency, and the IC_{50} value of compound **14** towards nNOS was 10 times lower than that of **6** (2.5 ± 0.5 μM). Interestingly, **14** was more selective of nNOS versus iNOS and eNOS than **12** (Table 1). Furthermore, another new indazole derivative, compound **8**, was even more selective towards nNOS versus iNOS and eNOS. It was half as potent as **6** towards nNOS (IC_{50} = 55 ± 10 μM) but was

Table 1. Effects of indazole derivatives **1–18** as inhibitors of purified recombinant NOS and on the visible spectrum of $nNOS_{oxy}$

Compound	Substituent	Inhibitory effects (IC_{50} values, μM)[a]			Visible spectra (λ_{max} in nm)[b]
		nNOS	iNOS	eNOS	
1	7-NO_2	25 ± 5	50 ± 10	35 ± 5	398
2	7-OH	700 ± 100	650 ± 125	700 ± 100	n.d.
3	7-OSO_2CF_3	500 ± 100	>1 mM (35%) [c]	>1 mM(45%)[c]	n.d.
4	7-NH_2	850 ± 100	110 ± 20	400 ± 80	n.d.[d]
5	7-I	200 ± 50	370 ± 80	125 ± 20	n.d.
6	7-CN	25 ± 8	110 ± 30	30 ± 8	398
7	7-CO_2H	>1 mM (35%)[c]	>1 mM (20%)[c]	>1 mM (40%)[c]	n.d.
8	7-$CONH_2$	55 ± 10	850 ± 150	500 ± 100	n.d.
9	7-(Tetrazol-5-yl)	>1 mM (15%)[c]	>1 mM (5%)[c]	>1 mM (30%)[c]	n.d.
10	7-C≡CH	>1 mM (30%)[c]	>1 mM (15%)[c]	225 ± 50	n.d.
11	7-(Triazol-5-yl)	>1 mM (45%)[c]	>1 mM (20%)[c]	>1 mM (45%)[c]	n.d.
12	3-Br-7-NO_2	1.8 ± 0.5	2.2 ± 0.6	2.0 ± 0.5	396[e]
13	3-Br-7-I	750 ± 50	900 ± 100	500 ± 100	n.d.
14	3-Br-7-CN	2.5 ± 0.5	5.7 ± 1.5	13 ± 3	398
15	3-Br-7-CO_2H	>1 mM (30%)[c]	700 ± 150	>1 mM (10%)[c]	n.d.
16	3-Br-7-$CONH_2$	>1 mM (35%)[c]	>1 mM (15%)[c]	>1 mM (45%)[c]	n.d.
17	1-CH_3-7-NO_2	700 ± 50	750 ± 50	250 ± 50	n.d.
18	1-CH_3-3-Br-7-NO_2	>500 (40%)[c]	>500 (15%)[c]	>500 (45%)[c]	n.d.

[a] IC_{50} values for the inhibition of purified recombinant n-, i-, or eNOS by compounds **1–18** were determined by monitoring the oxidation by NO of $HbFe^{II}O_2$ to $MetHbFe^{III}$ in incubations containing 10 μM L-arg and 10 μM H_4B (final concentrations), as described in Section 5. Specific activities for n-, i-, and eNOS were 350 ± 50, 800 ± 100, and 80 ± 30 nmol min^{-1} mg $protein^{-1}$, respectively. IC_{50} values are means ± SD from 4 to 6 experiments.

[b] Position of the maximum appearing in the difference spectrum obtained after addition of 100 μM compounds **1–18** to a solution of 1 μM $nNOS_{oxy}$ containing 1 mM ImH. This position is mentioned only for compounds leading to a significant difference spectrum. n.d., no appearance of a significant difference spectrum.

[c] Percent inhibitions observed at the highest concentration tested (500 μM or 1 mM).

[d] When added to native $nNOS_{oxy}$ (without ImH), this compound gave rise to a peak at 429 nm and a valley at 420 nm.

[e] Appearance of a broad difference spectrum obscured by the absorption of **12** itself.

inactive against iNOS and eNOS (IC_{50} = 850 and 500 μM, respectively).

All the other tested compounds, which bear an OH, OSO_2CF_3, NH_2, I, CO_2H, ethynyl, tetrazol-5-yl, or triazol-5-yl substituent at position 7 of the indazole ring, were very poor inhibitors of purified NOSs, with IC_{50} values between 200 μM and >1 mM. Introduction of a methyl group at the *N*(1) position of **1** and **12** led to a strong loss of the inhibitory effects (see compounds **17** and **18** in Table 1).

The inhibitory effects of compounds **1–18** were tested towards an inducible NOS expressed in a murine macrophage cell line.[40] Using the nitrite accumulation in the supernatant of LPS + γ-IFN-stimulated RAW 264.7 cells as a measure of iNOS activity,[41] compounds **1–11, 13, 15–18** were almost inactive (IC_{50} > 200 μM, data not shown). Only compound **12** and new compound **14** displayed significant inhibitory effects (IC_{50} = 80 ± 25 μM for both compounds) without noticeable cell toxicity. Further experiments using cell line expressing nNOS are under investigation.

3.2. Spectroscopic studies of the binding of the indazole derivatives 1–18 to $nNOS_{oxy}$

High resolution crystal structures of the complexes between **1** and **12** with the oxygenase domains of i- and eNOS (i- and $eNOS_{oxy}$) have shown that these inhibitors are bound at the active site and stacked parallel to the heme plane within van der Waals contact. This binding induces conformational changes with a displacement of a glutamate residue involved in L-arg binding from its usual position (Glu363, numbering from bovine eNOS).[27,28]

In order to compare the possible interactions of compounds **1–18** with the nNOS active site, we have studied their effects on the oxygenase domain of nNOS ($nNOS_{oxy}$) by differential UV–visible spectroscopy. The UV–visible spectrum of $nNOS_{oxy}$ in Hepes buffer, pH 7.4, displayed a broad Soret peak with a maximum at 415 nm indicating that $nNOS_{oxy}$ exists as a mixture of hexacoordinated heme–Fe^{III}–H_2O (low spin, LS) and pentacoordinated heme–Fe^{III} states (high spin, HS), the former state being predominant, in agreement with the literature data.[42] Addition of 1 mM imidazole (ImH) was done to completely convert $nNOS_{oxy}$ into a LS hexacoordinated heme–Fe^{III}–ImH complex absorbing at 430 nm. This method was very often used to more easily follow the binding of substrates to the NOS active site.[43] As previously described,[24] the stepwise addition of **1** to the $nNOS_{oxy}$–Fe^{III}–ImH complex gave rise to a difference spectrum characterized by a trough at 425 nm and a peak at 398 nm, showing that the binding of **1** close to the heme shifted the $nNOS_{oxy}$ spin state equilibrium to the HS pentacoordinated heme–Fe^{III} state (called Type 1 interaction) corresponding to a displacement of bound ImH.[43] Under identical conditions, the stepwise addition of **12** led to the appearance of a broad difference spectrum, which was difficult to analyze because of the absorption of the compound itself in the 380–420 nm region. By contrast, stepwise additions of **6** or **14** led to intense difference spectra almost identical to

that obtained with **1** (Table 1). All the other indazole derivatives tested led to very weak, not significant, difference spectra after addition either to native $nNOS_{oxy}$ or to $nNOS_{oxy}$–ImH complex (Table 1).

In order to confirm the strong binding of **6** to the $nNOS_{oxy}$ active site suggested by UV–visible spectroscopy, its effects on $nNOS_{oxy}$ spin state were followed by EPR spectroscopy at cryogenic temperatures. The X-band EPR spectrum of 25 μM $nNOS_{oxy}$ at 12 K (Fig. 1A) showed signals at $g = 7.60$, 4.10, and 1.870 corresponding to the HS heme–Fe^{III} complex, and broad signals which could correspond to mixtures of LS heme–Fe^{III} complexes ($g =$ 2.557, 2.512, 2.306 and 1.843).[44] Addition of 100 μM of **1** led to a dramatic change of the EPR spectrum with the appearance of an intense signal at $g =$ 7.49, 4.62, and 1.867, corresponding to a HS heme–Fe^{III} complex, clearly distinct from the native HS heme–Fe^{III} complex. Moreover, the features around $g =$ 2 corresponding to LS heme–Fe^{III} complexes were almost undetectable (Fig. 1B). Addition of 100 μM of **6** to $nNOS_{oxy}$ led to very similar results with the appearance of intense signals at $g =$ 7.45, 4.34 and 1.862 corresponding to a HS heme–Fe^{III} complex characterized by g-values close to those of the $nNOS_{oxy}$–**1** complex (Fig. 1C). As expected for HS heme–Fe^{III} complexes, an important decrease in intensity of the HS features was observed at 35 K (data not shown). By contrast, addition of compound **8** (200 μM) to $nNOS_{oxy}$ under identical conditions led to different EPR characteristics, with much less intense signals at *g*-values (7.57, 4.17, and 1.861) that were closer to those of native $nNOS_{oxy}$ (data not shown).

3.3. Mode of inhibition of nNOS by 6

On the basis of these results, we more deeply investigated the inhibition of nNOS by the new compound **6**. Kinetic studies of the inhibition of recombinant nNOS in the presence of 10 μM H_4B and various concentrations of substrate L-arg and **6** were carried out. Double-reciprocal plots of NO formation as a function of [L-arg] showed a change of the apparent K_m for nNOS-catalyzed oxidation of L-arg in the presence of **6** without significant effect on the apparent V_m (Fig. 2). These results indicated that nNOS was inhibited by **6** in a competitive manner versus L-arg. Replots of the apparent K_m for L-arg oxidation as a function of [**6**] led to an apparent K_i value of 13 μM for this inhibition under the conditions used in these experiments (Inset of Fig. 2).

The effects of H_4B concentration on the inhibition of nNOS-catalyzed oxidation of L-arg by **6** were studied

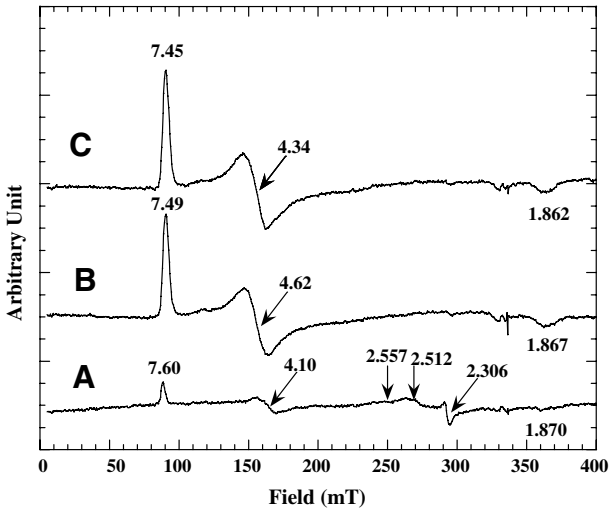

Figure 1. Effects of the addition of **1** or **6** on the EPR spectrum of purified $nNOS_{oxy}$. Line A, EPR spectrum of 25 μM native $nNOS_{oxy}$. Line B, EPR spectrum after the addition of 100 μM **1**. Line C, EPR spectrum after the addition of 100 μM **6**. Experimental conditions were as follows: sample temperature, 12 K; microwave power, 20 mW; modulation frequency, 100 kHz; modulation amplitude, 0.5 mT; averaged scans, 4; scan width, 0.5 T; center field, 0.255 T.

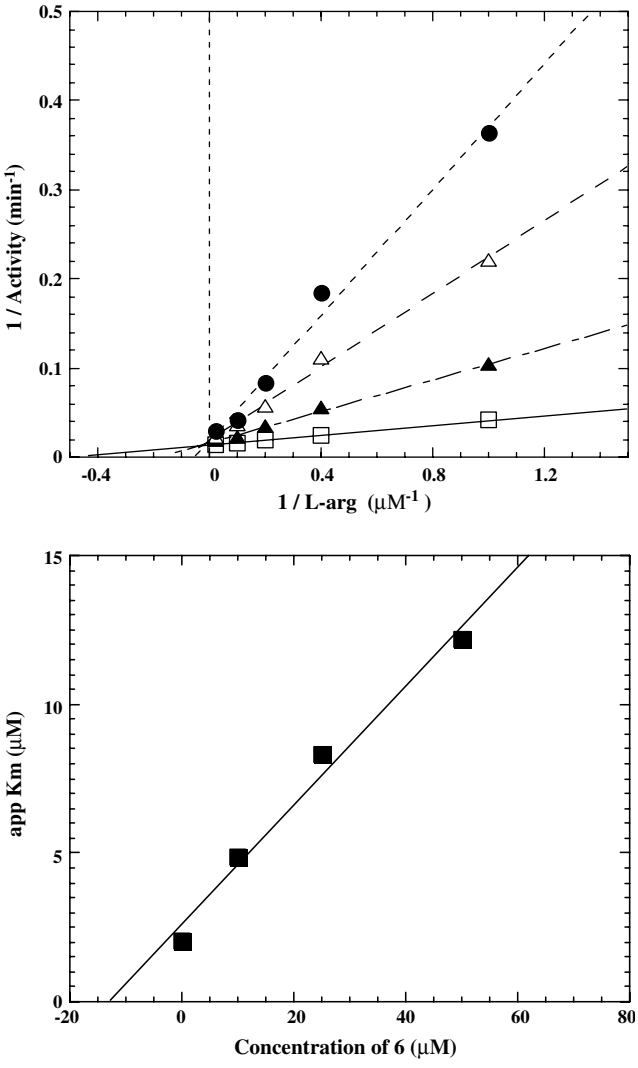

Figure 2. Effect of compound **6** on the apparent K_m value of nNOS-catalyzed oxidation of L-arg. Incubations were performed in the presence of 10 μM H_4B and the various concentrations of L-arg, without (□) or in the presence of 5 μM (▲), 25 μM (△), and 50 μM (●) of **6**. Incubations were initiated with the introduction of 20–40 nM nNOS and the oxidation of oxyhemoglobin to methemoglobin by NO formation was measured at 37 °C, as indicated in Section 5. Data are plotted in double-reciprocal format and are representative of a typical experiment. The inset shows the replot of apparent K_m values versus inhibitor concentrations.

from incubations of nNOS containing 10 μM L-arg and various concentrations of **6** and H_4B. Figure 3 shows that the IC_{50} for **6** was reduced 10-fold when [H_4B] decreased from 10 to 0.1 μM. These data suggested that **6** could compete with both the L-arg substrate and the H_4B cofactor in the nNOS active site, as previously found for **1**, **12**, and 7-methoxy-1*H*-indazole.[12,13,24,45,46] Finally, in order to check for the reversibility of the inhibition of nNOS by **6**, nNOS containing 10 μM H_4B, 100 μM NADPH, and CaM was preincubated for 5 min at 25 °C in the presence of 2.5 mM of **6**, a concentration 100-fold higher than its IC_{50} value. Then, the mixture was diluted 1000-fold and 10 μM L-arg was added. NO formation was measured and the activity was found to be not significantly different from that of a control experiment performed without **6** (data not shown).

Binding of substrates or inhibitors to the NOS active site can also alter the electron-transfer from the reductase to the heme. NADPH oxidase activity measures the effects of compounds on electron-transfer between the two domains of NOS, a process strongly dependent upon CaM binding.[47–49] As already described for this isoform,[47,49] NADPH oxidase activity of nNOS was half-reduced in the presence of 100 μM L-arg, and completely abolished in the presence of 10 μM NO_2-arg (data not shown). The addition of 10 μM of **6** or **14** to nNOS containing CaM completely reduced its NADPH oxidase activity (data not shown).

3.4. Molecular modeling analysis

Comparison of NOS inhibitory potencies between our new indazole derivatives and **12** can be rationalized on the basis of the X-ray structures published for the complexes of **1** and **12** bound to i- and eNOS.[27,28] Three key features have been identified (Fig. 4A). First, the indazole ring is positioned above the heme, making a π-stacking between the aromatic rings. Second, two H-bonds secure the position of the indazole ring: one between the indazole N(1)-*H* and the carbonyl O-atom of Trp358, and the second one between one O-atom of the nitro group and the peptide NH group of Met360. Finally, some hydrophobic stabilization of the 3-bromine atom fitted in an hydrophobic pocket delimited by Phe355, Gly357, Val 338, and the heme provides a large increase in affinity (Fig. 4A).[27,28] To analyze our data at a molecular level, we have superimposed the indazole ring of derivatives **2**–**11**, and **13**–**18**, to the indazole ring of **12** bound to eNOS. We could then evaluate if any of the three features listed above were still present for each derivative. Obviously, the π-stacking between the aromatic rings and the heme is always conserved. Comparison of IC_{50}'s of **1**, **5**–**7** with those of **12-15**, respectively, reveals a correlation between values of 7-monosubstituted and 3,7-disubstituted compounds.

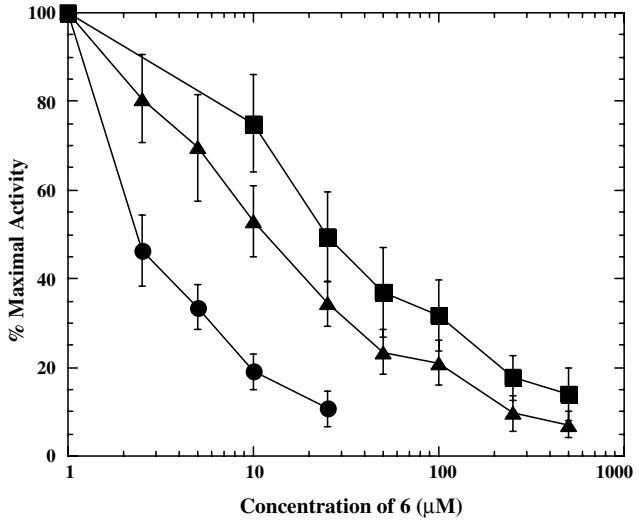

Figure 3. Effect of different H_4B concentrations on the inhibition of nNOS by **6**. Incubations were performed in the presence of 10 μM L-arg and 0.1 μM (●), 1 μM (▲) or 10 μM (■) H_4B. Incubations were initiated with the introduction of 20–40 nM nNOS and formation of NO was measured at 37 °C using the oxyhemoglobin assay, as indicated in Section 5. Activities of nNOS in the presence of 0.1, 1.0, and 10 μM H_4B were 65 ± 15, 310 ± 80, and 330 ± 50 nmol min^{-1} mg $protein^{-1}$, respectively.

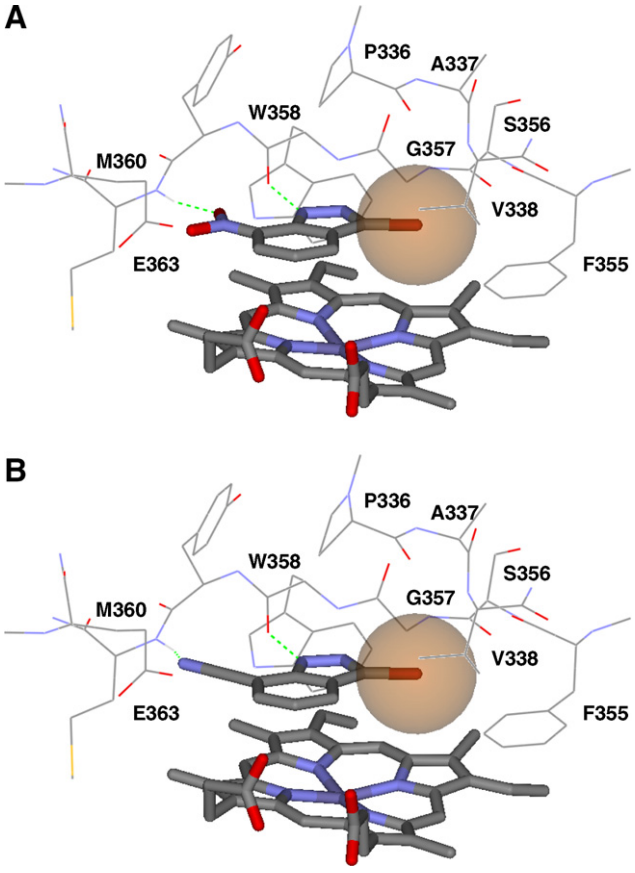

Figure 4. (A) Crystallographic structure of **12** bound at the active site of the oxygenase domain of eNOS (PDB access 1D0C). Heme and inhibitor **12** are displayed in boldsticks and hydrogen bonds as green dotted lines. A van der Waals sphere around the bromine atom shows how it is fitted into the hydrophobic pocket. Atom color code: carbon, gray; oxygen, red; nitrogen, blue; bromine, brown; sulfur, yellow. (B) Superimposition of **14** to the crystal structure of **12** bound to the oxygenase domain of eNOS. Visualization of crystallographic structures and superimposition were carried out using Discovery Studio 1.6 (Accelrys, San Diego).

For compounds **12** and **14**, a 10-fold decrease in IC_{50} values is observed by comparison to **1** and **6**. This suggests that the bromine atom of **13–15** is positioned in the same hydrophobic pocket as for **12** and can provide a similar stabilization. While the 3-bromo substitution is not essential, the two H-bonds between the inhibitor and Trp358 and Met360 are required for activity. Indeed, the *N*(1)-methyl substitution, in **17** and **18**, eliminates the binding to Trp358 and dramatically reduces the inhibition (Table 1). In compounds **2, 4, 5**, and **13**, the hydrogen bond to Met360 may not occur and inhibition is weakened although the interaction between the *N*(1)-*H* of indazoles and Trp358 is still present. The lack of activity of **9** and **11** could be due to the bulk of their substituents at the 7-position that could not be accomodated in that part of the binding site. On the other hand, in **6** and **14**, the cyano group could establish H-bonds with the Trp358 and Met360 residues very close to those observed with the nitro group of **1** and **12** (Fig. 4B). Unable to establish such H-bonds, compound **10** is inactive. Interestingly, when a carboxylic acid group is introduced in the 7-position, in compounds **7** and **15**, the activity is abolished (Table 1). This could be explained by the close proximity of the side chain of Glu363, a critical residue for NOS activity able to adopt various conformations, with a carboxylate function that should be predominantly in an anionic form. The distance between the negative charge of **7** or **15** and of Glu363 varies from 1.2 to 4.0 Å according to the different conformations. This results in an electrostatic repulsion that may be the cause of the loss of inhibitory effect. Such an argument would also explain the poor inhibitory effects of compound **9** that should be negatively charged at physiological pH. Such a repulsion should not occur in the case of compound **8** that bears a $CONH_2$ 7-substituent. This could explain the inhibitory effects of this compound. However, several data show that compounds **1** and **8** exhibit different behaviors toward nNOS: (i) contrary to **1**, **8** failed to produce any UV–visible difference spectrum after addition to $nNOS_{oxy}$, (ii) **1** and **8** led to clearly different EPR spectra with $nNOS_{oxy}$, and (iii) introduction of a 3-Br-substituent in **1** or **8** resulted in opposite effects on their IC_{50} values for inhibition of nNOS (i.e., a clear decrease in the case of **1** instead of a marked increase in the case of **8**, see Table 1). This suggests that the $CONH_2$ group of **8** may still interfere with the H-bonding network between the inhibitor and nNOS but with a somewhat distinct orientation. This could lead to a different positioning of the indazole heterocycle in the active site resulting in the inability of the bromine-atom to fit in the hydrophobic pocket described above. A factor that could be involved to explain these facts is the distinct electron-withdrawing ability of the NO_2 and CN groups compared to the $CONH_2$ group that might modify the π-stacking interactions involved between the indazole ring and the heme.

Altogether, our experimental results are in agreement with this simple molecular analysis that demonstrates that the three structural features identified for **12** must be simultaneously present for high NOS inhibition potency, as it is the case with the new compound **14**. Better understanding of these molecular structural differences between 7-substituted-1*H*-indazoles requires further crystallographic studies and will help in the search of more potent and selective inhibitors of nNOS with low toxicity.

4. Conclusion

In order to find substitutes for 7-nitro-1*H*-indazole as inhibitors of NOSs, we have synthesized six new indazole derivatives bearing different substituents at position 7 and four new 3,7-disubstituted derivatives. Among our series of fifteen indazole derivatives that were studied for the first time as inhibitors of purified n-, i-, and eNOS (compounds **3–11** and **13–18**), only three compounds, **6**, **8**, and **14**, acted as good inhibitors of the formation of NO ($IC_{50} < 100$ μM). Compounds **6** and **14** exhibit IC_{50} values similar to those of **1** and **12** (25 and 2 μM, respectively, Table 1) and compound **14** seems slightly more selective than **12** towards nNOS compared to iNOS and eNOS.

Even though compound **8** is interesting, as it is selective towards nNOS by comparison to i- and eNOS, it exhibits a very different behavior toward nNOS by comparison to **1**. On the contrary, compounds **1** and **6** exhibit very similar properties. Both are reversible inhibitors of NOS-catalyzed NO formation in a competitive manner versus both L-arg and H4B (Figs. 2 and 3),[12,13,45,46] and they inhibit electron-transfer from the reductase to the heme.[24] These results showed that **1** and **6** inhibit the catalytic activities that are catalyzed by the heme domain of nNOS. This was confirmed by our UV–visible and EPR studies using $nNOS_{oxy}$ that clearly indicated that binding of **1** and **6** to the $nNOS_{oxy}$ active site led to HS heme–Fe^{III} complexes exhibiting highly similar UV–visible and EPR characteristics (Fig. 1). Finally, another common feature between **1** and **6** resides in the strong enhancement of their inhibitory effects by further introduction of a bromine-atom at the 3-position of the heterocycle. Although bearing distinct substituents, **1** and **6** thus display close analogies between their mechanisms of inhibition and their binding modes.

New compounds **6** and **14** thus appear as good substitutes for **1** and **12**. They are as potent inhibitors of nNOS as **1** and **12**, and one may expect that they are less toxic than **1** and **12** since they do not have any nitro substituent. Further experiments are required to determine whether they keep the in vivo selectivity towards nNOS reported for **1** and to confirm that they are non-toxic.

5. Experimental

5.1. Chemistry—general procedures

7-Nitro-1*H*-indazole **1**, 3-bromo-7-nitro-1*H*-indazole **12**, and *N*-(2-pyridyl) bis(trifluoromethanesulfonimide) were purchased from Aldrich. All other commercially available chemicals and reagents were purchased from Sigma or Acros and were used without further purification. 1*H*-Indazol-7-ol **2** was obtained from

7-methoxy-1*H*-indazole by treatment with BBr_3 in CH_2Cl_2 following a previously described protocol.[22] Organic solvents were distilled from a drying agent prior to use following usual methods. Chemical reactions were monitored by analytical TLC using Merck precoated silica gel $60F_{254}$ plates. Flash chromatography was performed on silica gel 60 (particle size 35–70 μm) supplied by SDS. Melting points were determined on a Büchi B-445 melting point apparatus and are uncorrected. ^1H, ^{13}C, and ^{19}F NMR spectra were recorded in commercial deuterated solvents on Bruker AC 200 or Advance 300 spectrometers. Chemical shifts are reported in parts per million (δ) relative to tetramethylsilane with peak multiplicities abbreviated as follows: singlet, s; broad singlet, br s; doublet, d; triplet, t; multiplet, m. Coupling constants, *J*, are reported in Hz. Chemical shifts for ^{19}F NMR spectra are relative to $CFCl_3$. Infra-red spectra were recorded on a Nicolet Opus-IR spectrometer with samples prepared as pellets mixed with KBr. Mass spectra were recorded on a GC-MS HP-5989B spectrometer (ILV, Versailles, France). High resolution mass spectra were recorded on a Jeol MS700 spectrometer (ENSCP, Paris, France). Elemental analyses were performed at Service de Microanalyse ICSN-CNRS (Gif sur Yvette, France).

5.1.1. 1*H*-Indazol-7-yl trifluoromethanesulfonate (3). To a solution of 1*H*-indazol-7-ol **2** (20.0 mg, 0.149 mmol) in 15 mL of THF containing Cs_2CO_3 (29.0 mg, 0.089 mmol) and K_2CO_3 (20.6 mg, 0.149 mmol), *N*-(2-pyridyl)bis(trifluoromethane sulfonimide) (53.4 mg, 0.149 mmol) was added at −10 °C.[29]The resulting mixture was stirred at room temperature for 2 h and the solvent was evaporated. The product was extracted with CH_2Cl_2, washed with water, 5% HCl, and brine. After drying on $MgSO_4$, the solvent was evaporated in vacuo to afford **3** (38.0 mg, 96%) as a brown powder. Mp: 94 °C. ^1H NMR (200 MHz, acetone-d_6) δ 7.27 (t, 1H, $J = 9.2$), 7.50 (d, 1H, $J = 9.2$), 7.93 (d, 1H, $J = 9.2$), 8.27 (s, 1H). ^{19}F NMR (188 MHz, acetone-d_6) δ −68.92 (s, 3F). ^{13}C NMR (75 MHz, acetone-d_6) δ 115.8, 116.5, 119.0, 119.4, 121.8, 122.5, 122.9, 128.3. MS (CI_{CH4}) *m*/*z* 267 ($M+H^+$). HRMS Calcd for $C_8H_5N_2F_3O_3S$ ($M + NH_4^+$): 267.0051. Found: 267.0056.

5.1.2. 1*H*-Indazol-7-amine (4). To a solution of **1** (5.00 g, 30.6 mmol) in EtOH (200 mL) containing 98 mg of Pd on activated carbon was added ammonium formate (25.1 g, 398 mmol). The solution was refluxed with vigorous stirring for 1 h. The catalyst was removed by filtration and the solvent evaporated in vacuo. The product was extracted with ethyl acetate, washed with water and brine. After drying on $MgSO_4$, the solution was evaporated in *vacuo* to afford 3.06 g (75 %) of **4** as a brown powder. Mp: 159 °C (162 °C).[50] ^1H NMR (200 MHz, $CDCl_3$) δ 5.80 (br s, 2H, NH_2), 6.67 (d, 1H, $J = 7.6$), 7.01 (t, 1H, $J = 7.6$), 7.24 (2d, 2H, $J = 7.6$), 8.08 (s, 1H). ^{13}C NMR (75 MHz, $CDCl_3$) δ 110.8, 111.6, 122.2, 124.2, 130.6, 133.0, 134.8. MS (EI) *m*/*z* 133 (M^+).

5.1.3. 7-Iodo-1*H*-indazole (5). To a cooled solution of **4** (300.0 mg, 2.25 mmol) in concentrated HCl (0.56 mL) and 98% H_2SO_4 (2 mL) was added dropwise a solution of $NaNO_2$ (154.0 mg, 2.23 mmol) in 1 mL of water. The mixture was stirred vigorously at 0 °C for 40 min. Then, a solution of KI (747.0 mg, 4.500 mmol) in 0.9 mL of water was added dropwise and the mixture was stirred at room temperature for 2 h. The product was extracted with ethyl acetate, washed with a saturated sodium carbonate solution, water and brine. After drying on $MgSO_4$, the solution was concentrated in vacuo. The crude product was purified by column chromatography on silica gel, eluting with diethyl ether/pentane (2:3) to afford 394.0 mg (71 %) of **5** as a brown powder. Mp: 114 °C. ^1H NMR (200 MHz, $CDCl_3$) δ 6.97 (t, 1 H, $J = 7.5$), 7.55 (br s, 1H, NH), 7.73 and 7.77 (2d, 2H, $J = 7.5$), 8.25 (s, 1H). ^{13}C NMR (75 MHz, $CDCl_3$) δ 115.7, 121.0, 122.7, 123.2, 135.6, 136.2, 142.4. MS (EI) *m*/*z* 117 ($M-I)^+$, 127 ($I^{+\cdot}$), 244 (M^+). Anal. Calcd for $C_7H_5N_2I$: C 34.43, H 2.05, N 11.47, Found: C 34.46, H 1.93, N 11.38.

5.1.4. 1*H*-Indazole-7-carbonitrile (6). A flask flushed with argon was charged with **5** (500.0 mg, 2.05 mmol), 1,1′-bis(diphenylphosphino)ferrocene (dppf, 90.0 mg, 0.16 mmol, 7.8 mol %), tris(dibenzylideneacetone)dipalladium ($Pd_2(dba)_3$, 75.0 mg, 0.082 mmol, 4.0 mol %), zinc powder (32.0 mg, 0.490 mmol), and $Zn(CN)_2$ (144.0 mg, 1.23 mmol). Degassed *N*,*N*-dimethylacetamide (40 mL) was added, and the resulting mixture was heated at 120 °C with vigorous stirring for 4 h. The reaction mixture was concentrated under vacuum and diluted with ethyl acetate. The organic layer was washed with 2 N NH_4OH and brine, dried on $MgSO_4$, and concentrated in *vacuo*. The crude product was purified by chromatography on silica gel, eluting with diethyl ether/pentane (2:3) to afford 190.0 mg (63%) of **6** as a white powder. Mp: 160 °C. IR (KBr) 2218 cm^{-1}. ^1H NMR (200 MHz, acetone-d_6) δ 7.32 (t, 1 H, $J = 13.3$), 7.87 (d, 1H, $J = 13.3$), 8.18 (d, 1H, $J = 13.3$), 8.28 (s, 1H), 13.14 (br s, NH). ^{13}C NMR (75 MHz, acetone-d_6) δ 94.9, 116.9, 121.5, 125.2, 127.5, 132.8, 135.5, 136.2. MS (EI) *m*/*z* 143 (M^+). Anal. Calcd for $C_8H_5N_3$: C 67.13, H 3.50, N 29.37. Found: C 67.14, H 3.71, N 29.28.

5.1.5. 1*H*-Indazole-7-carboxylic acid (7). A flask was charged with **6** (100 mg, 0.698 mmol) in 6 N HCl (8 mL) and the resulting mixture was refluxed for 12 h. The white precipitate was filtered, washed with cold water and dried in *vacuo* to afford **7** (111 mg, 98%) as a white powder. Mp: 225 °C (230–233 °C).[33] ^1H NMR (200 MHz, DMSO-d_6) δ 7.23 (t, 1H, $J = 6.6$), 7.97 (d, 1H, $J = 6.6$), 8.06 (d, 1H, $J = 6.6$), 8.20 (s, 1H), 9.85 and 13.12 (2 br s, NH and COOH). ^{13}C NMR (75 MHz, DMSO-d_6) δ 113.6, 119.9, 124.5, 126.3, 128.7, 134.1, 137.8, 166.8. MS (ESI negative mode) *m*/*z* 161 ($M-H^-$). HRMS Calcd for $C_8H_7N_2O_2$ $(M+H)^+$: 163.0508. Found: 163.0504.

5.1.6. 1*H*-Indazole-7-carboxamide (8). To a solution of **7** (140 mg, 0.863 mmol) and NEt_3 (0.260 mL, 1.87 mmol) dissolved in CH_2Cl_2 (13 mL), ethyl chloroformate (95 μL, 0.99 mmol; 1.1 equiv) was added at −20 °C. The mixture was stirred for 40 min and NH_3 was then

slowly bubbled for 10 min at −20 °C. The reaction mixture was poured into water and the product extracted with CH_2Cl_2. The organic layer was washed with water, 1 N HCl, brine, dried over $MgSO_4$ and evaporated to dryness in vacuo. The product was purified by column chromatography on silica gel, eluting with CH_2Cl_2/EtOH (98:2), to afford **8** (128 mg, 92%) as a white powder. Mp: 136 °C. ^{1}H NMR (200 MHz, acetone-d_6) δ 5.70 (br s, 2H), 7.21 (t, 1H, J = 7.2), 7.97 (2d, 2H, J = 7.2), 8.11 (s, 1H), 12.25 (br s, 1H). ^{13}C NMR (75 MHz, acetone-d_6) δ 115.0, 120.7, 124.1, 124.6, 125.6, 125.9, 135.9, 168.1. MS (EI) *m/z* 161 (M^+). HRMS Calcd for $C_8H_8N_3O$ ($M+H^+$): 162.0663. Found: 162.0667.

5.1.7. 7-(1*H*-Tetrazol-5-yl)-1*H*-indazole (9). A solution of **6** (100 mg, 0.69 mmol) in 10 mL of toluene was added dropwise to a solution of trimethylsilylazide (0.110 mL, 0.83 mmol) and trimethylaluminum (2.0 M in toluene, 0.420 mL, 0.84 mmol) in 2 mL of toluene at 0 °C. The yellow mixture was stirred for 30 min at room temperature and then for 48 h at 80 °C. After cooling to 0 °C, the mixture was poured into a biphasic mixture of 6 mL of ethyl acetate and 6 mL of 6 M HCl. The product was extracted with ethyl acetate and the combined organic layers were washed with water and brine, dried over $MgSO_4$ and evaporated under vacuum. Purification by column chromatography on silica gel, eluting with ethyl acetate/petroleum ether (1:1), afforded **9** (30.0 mg, 23%) as a brown powder. Mp: 320 °C. ^{1}H NMR (200 MHz, acetone-d_6) δ 3.72 (br s, 1H) 7.17 (t, 1H, J = 7.9), 7.72 (d, 1H, J = 7.9), 8.12 (s, 1H), 8.21 (d, 1H, J = 7.9), 12.52 (br s, 1H). ^{13}C NMR (75 MHz, acetone-d_6) δ 119.0, 120.0, 121.2, 123.0, 124.3, 124.5, 134.0, 163.5. MS (CI-NH_3) *m/z* 187 ($M+H^+$). HRMS Calcd for $C_8H_7N_6$ ($M+H^+$): 187.0732. Found: 187.0757.

5.1.8. 7-Ethynyl-1*H*-indazole (10). A Schlenk flask was charged with **5** (2.0 g, 8.2 mmol), tetrakis(triphenylphosphine)palladium ($Pd(PPh_3)_4$, 946 mg, 0.819 mmol, 10 mol %), and CuI (458.0 mg, 2.405 mmol). The flask was flushed with argon, and degassed CH_3CN (30 mL), trimethylsilylacetylene (1.4 mL, 10 mmol), and NEt_3 (5 mL) were added. The orange mixture was stirred for 6 hours at room temperature. The solution was evaporated, and the product was extracted with ethyl acetate. The organic layer was washed with water, brine, dried over $MgSO_4$ and evaporated in vacuo to afford crude 7-((trimethylsilyl)ethynyl)-1*H*-indazole **19** (1.23 g, 70 %) as a yellow oil that was used directly in the next step. ^{1}H NMR (200 MHz, $CDCl_3$) δ 0.32 (s, 9H), 7.13 (t, 1H, J = 8.1), 7.51 and 7.74 (2d, 2H, J = 8.1), 8.10 (s, 1H). Potassium carbonate (570 mg, 4.12 mmol) was added to a solution of crude **19** (880 mg, 4.10 mmol) in 250 mL MeOH, and the mixture was stirred for 16 hours at room temperature. The solvent was evaporated, and the product was extracted with ethyl acetate. The organic layer was washed with water and brine, dried over $MgSO_4$ and evaporated to dryness *in vacuo*. Purification by column chromatography on silica gel, eluting with ethyl acetate/pentane (1:4), afforded **10** (337 mg, 60%) as brown needles. Mp: 77 °C. IR (KBr) 3280, 2190 cm^{-1}. ^{1}H NMR (200 MHz, $CDCl_3$) δ 3.46 (s, 1H), 7.15 (t, 1H, J = 7.7), 7.56 (d, 1H, J = 7.7), 7.78 (d, 1H, J = 7.7), 8.15 (s, 1H), 10.70 (br s, 1H). ^{13}C NMR (75 MHz, $CDCl_3$) δ 79.2, 82.5, 104.4, 121.1, 122.1, 122.8, 130.8, 134.0, 143.5. MS (EI) *m/z* 142 (M^+). HRMS Calcd for $C_9H_7N_2$ ($M+H^+$): 143.0609. Found: 143.0620.

5.1.9. 7-(1*H*-[1,2,3]Triazol-5-yl)-1H-indazole (11). A sealed tube was charged with **10** (100 mg, 0.703 mmol), CuI (6.7 mg, 0.035 mmol; 0.050 eq), MeOH (0.5 mL), and DMF (4.5 mL). Trimethylsilylazide (0.140 mL, 1.0 mmol) was added and the mixture was heated at 120 °C for 48 h. The solvents were evaporated in vacuo to afford a brown oil. Purification by column chromatography on silica gel, eluting with ethyl acetate/petroleum ether (1:1) afforded **11** (125.0 mg, 96 %) as a yellow powder. Mp: 211 °C. ^{1}H NMR (200 MHz, acetone-d_6) δ 2.96 (s, 1H), 4.04 (s, 1H), 7.25 (t, 1H, J = 7.5), 7.82 (d, 1H, J = 7.5), 7.90 (d, 1H, J = 7.5), 8.15 (s, 1H), 12.40 (br s, 1H). ^{13}C NMR (75 MHz, acetone-d_6) δ 121.5, 121.6, 121.7, 123.9, 125.3, 129.6, 132.0, 133.5, 137.9. MS (CI-NH_3) m/z 186 ($M+H^+$). HRMS Calcd for $C_9H_8N_5$ ($M+H^+$): 186.0780. Found: 186.0801.

5.1.10. 3-Bromo-7-iodo-1*H*-indazole (13). *N*-Bromosuccinimide (730 mg, 4.10 mmol) and NaOH (170 mg, 4.25 mmol) were added to a solution of **5** (1.0 g, 4.10 mmol) in DMF (50 mL). The yellow mixture was stirred for 48 hours at room temperature. After addition of water, the product was extracted with ethyl acetate. The combined organic layers were washed with water and brine, dried over $MgSO_4$ and concentrated in vacuo. The crude mixture was purified by column chromatography on silica gel eluting with diethyl ether/petroleum ether (1:1) to afford **13** (1.04 g, 79%) as a white powder. Mp: 161 °C. ^{1}H NMR (200 MHz, $CDCl_3$) δ 7.03 (t, 1H, J = 8.0), 7.63 (d, 1H, J = 8.0), 7.81 (d, 1H, J = 8.0), 10.10 (br s, 1H). ^{13}C NMR (75 MHz, $CDCl_3$) δ 112.2, 120.4, 123.5, 124.3, 131.1, 136.7, 143.1. MS (EI) *m/z* 323 (M^+), 243 $(M\text{-}Br)^+$, 116 $(M–Br–I)^+$. Anal. Calcd for $C_7H_4N_2BrI$: C 26.01, H 1.24, N 8.67, Found: C 26.23, H 1.28, N 8.61.

5.1.11. 3-Bromo-1*H*-indazole-7-carbonitrile (14). Treatment of a solution of **6** (20.0 mg, 0.140 mmol) in DMF (5 mL) with *N*-bromosuccinimide (24.8 mg, 0.139 mmol) and NaOH (5.6 mg, 0.14 mmol) for 5 hours at room temperature was performed as described above for compound **13**. Purification of the crude product by column chromatography on silica gel eluting with diethyl ether/petroleum ether (1:1), afforded **14** (23.0 mg, 74%) as a white powder. Mp: 238 °C. IR (KBr) 2230 cm^{-1}. ^{1}H NMR (200 MHz, acetone-d_6) δ 7.45 (t, 1H, J = 6.9), 8.00 (d, 2H, J = 6.9), 13.30 (br s, 1H). ^{13}C NMR (75 MHz, acetone-d_6) δ 95.5, 116.1, 122.6, 123.7, 124.7, 126.3, 134.3, 141.3. MS (EI) *m/z* 221 (M^+), 142 $(M–Br)^+$. Anal. Calcd for $C_8H_4N_3Br$: C 43.24, H 1.80, N 18.92. Found: C 42.81, H 1.67, N 18.25.

5.1.12. 3-Bromo-1*H*-indazole-7-carboxylic acid (15). A mixture of **14** (29.0 mg, 0.131 mmol) in 10 N HCl (7 mL) was refluxed for 48 hours. After cooling to room temperature, the white precipitate was filtered, washed

with cold water and dried in vacuo to afford **15** (27.0 mg, 86 %) as a white powder. Mp: 280 °C. ^{1}H NMR (200 MHz, DMSO-d_6) δ 3.91 (br s, 1H), 7.35 (t, 1H, J = 7.3), 7.87 (d, 1H, J = 7.3), 8.06 (d, 1H, J = 7.3), 13.47 (s, 1H). ^{13}C NMR (75 MHz, DMSO-d_6) δ 114.4, 121.1, 121.4, 123.7, 124.8, 130.2, 139.0, 166.2. MS (ESI negative mode) m/z 241 $(M–H)^-$, 197 $(M–CO_2–H)^-$, 115 $(M–CO_2–Br–H)^-$. Anal. Calc. for $C_8H_5N_2O_2Br$: C 39.83, H 2.07, N,11.62. Found: C 39.87, H 1.97, N 12.11.

5.1.13. 3-Bromo-1*H*-indazole-7-carboxamide (16). To a cooled solution (−20 °C) of **15** (440 mg, 1.83 mmol) and NEt_3 (0.540 mL, 3.87 mmol) in CH_2Cl_2 (13 mL) was added ethyl chloroformate (0.200 mL, 2.10 mmol). The mixture was stirred for 40 min. Then, ammonia was slowly bubbled through the mixture for 10 min at −20 °C. The reaction mixture was poured into water and the product was extracted with CH_2Cl_2. The organic layer was washed with water, 1 N HCl, brine, dried over $MgSO_4$ and evaporated to dryness in vacuo. The product was purified by column chromatography on silica gel, eluting with CH_2Cl_2/ethanol (98:2), to afford **16** (414 mg, 95%) as a white powder. Mp: 287 °C. ^{1}H NMR (200 MHz, acetone-d_6) δ 7.18 (t, 1H, J = 6.3), 7.50 (br s, 2H), 7.53 (d, 1H, J = 6.3), 7.81 (d, 1H, J = 6.3), 12.25 (br s, 1H). ^{13}C NMR (75 MHz, acetone-d_6) δ 120.3, 120.5, 120.6, 120.9, 122.7, 128.4, 140.3, 168.5. MS (EI) m/z 239 (M^+). HRMS Calc for $C_8H_7N_3OBr$ $(M+H^+)$: 239.9772. Found: 239.9773.

5.1.14. 1-Methyl-7-nitro-1*H*-indazole (17). KOH (56 mg, 1.0 mmol) and CH_3I (0.150 mL, 2.4 mmol) were added to a solution of **1** (163 mg, 1.0 mmol) in acetone (5 mL) at 0 °C. After stirring for 3 hours at room temperature, the solution was evaporated. The crude product was dissolved in CH_2Cl_2, washed with water, brine, dried over $MgSO_4$, and the solvent was evaporated in vacuo. The residue was purified by column chromatography on silica gel, eluting with diethyl ether/cyclohexane (1:1), to afford **17** (156 mg, 88%) as a yellow powder. Mp: 100 °C (99–100 °C).[36] ^{1}H NMR (200 MHz, acetone-d_6) δ 4.24 (s, 3H), 7.35 (t, 1H, J = 7.9), 8.16 (d, 1H, J = 7.9), 8.21 (d, 1H, J = 7.9), 8.30 (s, 1H).

5.1.15. 3-Bromo-1-methyl-7-nitro-1*H*-indazole (18). A solution of **12** (182 mg, 0.752 mmol) in acetone (3 mL) was treated by CH_3I (0.120 mL, 1.9 mmol) in the presence of the KOH (45 mg, 0.80 mmol) following the protocol described above for **17**. Compound **18** (154 mg, 80%) was obtained as a yellow powder. Mp: 158 °C (160–162 °C).[36] ^{1}H NMR (200 MHz, $CDCl_3$) δ 4.26 (s, 3H), 7.32 (t, 1H, J = 7.6), 7.95 (d, 1H, J = 7.6), 8.22 (d, 1H, J = 7.6).

5.2. Biochemistry

5.2.1. General procedures. L-Arginine, L-citrulline, N^{ω}-nitro-L-arginine, dithiothreitol (DTT), hemoglobin, superoxide dismutase (SOD), catalase, bovine serum albumin, and porcine brain calmodulin were purchased from Sigma. (6*R*)-5,6,7,8-Tetrahydrobiopterin and 7-NI were purchased from Alexis (Coger, France) and NADPH from Boehringer. Recombinant nNOS was isolated and purified from the yeast *Saccharomyces cerevisiae* transformed with a plasmid containing rat brain nNOS as previously described.[51] Full length recombinant murine iNOS,[52] bovine eNOS,[53] and the heme domain of rat brain nNOS ($nNOS_{oxy}$)[42] were expressed in *Escherichia coli* and purified in the absence of H_4B and L-arg as described previously. Protein concentrations were determined by the method of Bradford using bovine serum albumin as a standard and the Bradford reagent from Biorad.[54] The heme concentrations of NOS were determined optically from the $[Fe^{II}$-CO]– $[Fe^{II}]$ difference spectrum using a $\Delta\varepsilon_{445-480\ nm}$ of 74 $mM^{-1}\ cm^{-1}$.[55] They were estimated to be more than 95% pure by SDS–PAGE electrophoresis.

5.2.2. Oxyhemoglobin assay. The rates of NO synthesis were determined at 37 °C on an Uvikon 941 spectrophotometer using the oxyhemoglobin assay for NO.[39] Usual incubation mixtures were performed in 1-cm path length cuvettes (total volume 150 µL) containing 50 mM Hepes buffer (pH 7.4) with 0.1 M KCl supplemented with DTT (5 mM), oxyhemoglobin (10-20 µM), 1000 U/mL each of SOD and catalase, 10 µM each of H_4B and L-arg, $CaCl_2$ (1 mM), CaM (10 µg/mL), NADPH (1 mM), and inhibitors. Compounds **1–18** were added to the incubation mixtures as 1.5 µL solutions in DMSO. The mixtures were preincubated for 2 min at 37 °C prior to initiation of the reaction by the addition of 2–5 µL aliquots of NOS to the sample cuvettes. The NO-mediated conversion of oxyhemoglobin to methemoglobin was monitored by repetitive scanning between 380 and 480 nm every 0.2 min, and quantitated using an extinction coefficient of 77 $mM^{-1}.cm^{-1}$ between peak at 401 nm and valley at 420 nm.[39] The production of NO was linear over all the entire reaction time for each isoform. Control incubations contained similar amounts (1%) of DMSO without inhibitor. All values are expressed relative to the DMSO control and as means ± SD from 3–4 experiments.

5.2.3. NADPH oxidation by nNOS. The effects of compounds **1–18** on the initial rates of NADPH oxidation by nNOS were quantitated spectrophotometrically using an extinction coefficient of 6.2 $mM^{-1}\ cm^{-1}$ for the decrease in absorbance at 340 nm, as previously described.[24]

5.3. Spectroscopic studies

5.3.1. UV–visible spectroscopy. Optical spectra were recorded at room temperature in 1-cm path length cuvettes containing 0.8–1.0 µM $nNOS_{oxy}$ in 150 µL of 50 mM Hepes pH 7.4. In some assays, ImH (1 mM) was added to $nNOS_{oxy}$ to form the LS-heme Fe^{III}-ImH complex. The baseline between 380 and 500 nm was recorded and stepwise additions of the assayed compounds dissolved in DMSO were performed. Equivalent amounts of DMSO (maximal 2%) were added to the reference cuvette.

5.3.2. EPR spectroscopy. EPR spectra were recorded on a Bruker Elexsys E500 EPR spectrometer operating at X-band frequency (9.45 GHz) equipped with an shq

0011 cavity and an Oxford Instrument liquid helium probe. The following instrument settings were used: modulation frequency, 100 kHz; modulation amplitude, 0.5 mT; time constant, 0.02 s; field sweep, 100 mT/min; center field, 255 mT. Quartz tubes containing native $nNOS_{oxy}$ (60 μL, 20–25 μM) or $nNOS_{oxy}$ containing the studied compounds were frozen in cold ethanol and then in liquid nitrogen. All spectra were recorded at 12 ± 2 K and 35 ± 2 K, with four accumulations for each experiment.

5.4. Effects of compounds 1–18 on NO synthase activity in RAW 264.7 cells

The murine macrophage RAW 264.7 cells were plated at 100,000 cells/well in 96-well plates in 200 μL of RPMI 1640 culture medium supplemented with 5% FCS and antibiotics, and incubated for 24 h at 37 °C under a 5% CO_2 atmosphere.[40] Fresh medium and various concentrations of compounds **1–18** were added 1 h before the addition of 40 U/mL γ-IFN and 50 ng/mL LPS. After incubation for 20 h at 37 °C, 100 μL of the supernatants were analyzed for nitrite formation using Griess' reagent (1% sulfanilamide and 0.1% 1-naphthyl-ethylenediamine in 0.5 M HCl) and absorbance at 550 nm was measured on a Victor plate reader.[41] Quantitation of nitrite formation was performed with calibration curves using known amounts of $NaNO_2$ treated under the same conditions.

Acknowledgments

B.C. acknowledges the Ministère de l'Education Nationale et de la Recherche for a fellowship. The authors thank M.-A. Sari, and M. Jaouen (UMR 8601 CNRS, Paris, France), and D. Durrad (Cleveland Clinic, Cleveland, USA) for their help in preparing proteins and performing electrophoresis.

References and notes

1. Kerwin, J. F.; Lancaster, J. R.; Feldman, P. F. *J. Med. Chem.* **1995**, *38*, 4343–4362.
2. Pfeiffer, S.; Mayer, B.; Hemmens, B. *Angew. Chem., Int. Ed.* **1999**, *38*, 1714–1731.
3. Davis, K. L.; Martin, E.; Turko, I. V.; Murad, F. *Annu. Rev. Pharmacol. Toxicol.* **2001**, *41*, 203–236.
4. Masters, B. S. S.; McMillan, K.; Sheta, E. A.; Nishimura, J. S.; Roman, L. J.; Martasek, P. *FASEB J.* **1996**, *10*, 552–558.
5. Alderton, W. K.; Cooper, C. E.; Knowles, R. G. *Biochem. J.* **2001**, *357*, 593–615.
6. Li, H.; Poulos, T. L. *J. Inorg. Biochem.* **2005**, *99*, 293–305.
7. Southan, G. J.; Szabo, C. *Biochem. Pharmacol.* **1996**, *51*, 383–394.
8. Babu, B. R.; Griffith, O. W. *Curr. Opin. Chem. Biol.* **1998**, *2*, 491–500.
9. Tinker, A. C.; Wallace, A. V. *Curr. Top. Med. Chem.* **2006**, *6*, 77–92.
10. Frey, C.; Narayanan, K.; McMillan, K.; Spack, L.; Gross, S. S.; Masters, B. S.; Griffith, O. W. *J. Biol. Chem.* **1994**, *269*, 26083–26091.
11. Flinspach, M. L.; Li, H.; Jamal, J.; Yang, W.; Huang, H.; Hah, J. M.; Gomez-Vidal, J. A.; Litzinger, E. A.; Silverman, R. B.; Poulos, T. L. *Nat. Struct. Mol. Biol.* **2004**, *11*, 54–59.
12. Wolff, D. J.; Gribin, B. J. *Arch. Biochem. Biophys.* **1994**, *311*, 300–306.
13. Wolff, D. J.; Lubeskie, A.; Umansky, S. *Arch. Biochem. Biophys.* **1994**, *314*, 360–366.
14. Blasko, E.; Glaser, C. B.; Devlin, J. J.; Xia, W.; Feldman, R. I.; Polokoff, M. A.; Phillips, G. B.; Whitlow, M.; Auld, D. S.; McMillan, K.; Ghosh, S.; Stuehr, D. J.; Parkinson, J. F. *J. Biol. Chem.* **2002**, *277*, 295–302.
15. Paige, J. S.; Jaffrey, S. R. *Curr. Top. Med. Chem.* **2007**, *7*, 97–114.
16. Moore, P. K.; Wallace, P.; Gaffen, Z.; Hart, S. L.; Babbedge, R. C. *Br. J. Pharmacol.* **1993**, *110*, 219–224.
17. Babbedge, R. C.; Bland-Ward, P. A.; Hart, S. L.; Moore, P. K. *Br. J. Pharmacol.* **1993**, *110*, 225–228.
18. Bland-Ward, P. A.; Moore, P. K. *Life Sci.* **1995**, *57*, PL131–PL135.
19. Boelsterli, U. A.; Ho, H. K.; Zhou, S.; Leow, K. Y. *Curr. Drug Metab.* **2006**, *7*, 715–727.
20. Purohit, V.; Basu, A. K. *Chem. Res. Toxicol.* **2000**, *13*, 673–692.
21. Boulouard, M.; Schumann-Bard, P.; Butt-Gueulle, S.; Lohou, E.; Stiebing, S.; Collot, V.; Rault, S. *Bioorg. Med. Chem. Lett.* **2007**, *17*, 3177–3180.
22. Schumann, P.; Collot, V.; Hommet, Y.; Gsell, W.; Dauphin, F.; Sopkova, J.; MacKenzie, E. T.; Duval, D.; Boulouard, M.; Rault, S. *Bioorg. Med. Chem. Lett.* **2001**, *11*, 1153–1156.
23. Collot, V.; Sopkova, J.; Schumann-Bard, P.; Colloc'h, N.; MacKenzie, E. T.; Rault, S. *J. Enzyme Inhib. Med. Chem.* **2003**, *18*, 195–199.
24. Tuynman, A.; Perollier, C.; Frapart, Y.; Schumann-Bard, P.; Collot, V.; Rault, S.; Boucher, J. L. *Nitric Oxide* **2003**, *9*, 86–94.
25. Sopkova, J.; Collot, V.; Rault, S. *Acta Crystallogr.* **2000**, *C56*, 1503–1504.
26. Sopkova-De Oliveira Santos, J.; Collot, V.; Rault, S. *Acta Crystallogr.* **2002**, *C58*, 688–690.
27. Raman, C. S.; Li, H.; Martasek, P.; Southan, G.; Masters, B. S. S.; Poulos, T. L. *Biochemistry* **2001**, *40*, 13448–13455.
28. Rosenfeld, R. J.; Garcin, E. D.; Panda, K.; Andersson, G.; Aberg, A.; Wallace, A. V.; Morris, G. M.; Olson, A. J.; Stuehr, D. J.; Tainer, J. A.; Getzoff, E. D. *Biochemistry* **2002**, *41*, 13915–13925.
29. Comins, D. L.; Dehghani, A. *Tetrahedron Lett.* **1992**, *33*, 6299–6302.
30. Ram, S.; Ehrenkaufer, R. E. *Tetrahedron Lett.* **1984**, *25*, 3415–3418.
31. Cottyn, B.; Vichard, D.; Terrier, F.; Nioche, P.; Raman, C. S. *Synlett* **2007**, 1203–1207.
32. Xie, W.; Herbert, B.; Schumacher, R.; Nguyen, T. M.; Ma, J.; Gauss, C. M; Tehim, A. PCT Int. Appl. WO 2005092890, 2005.
33. Barber, C. G.; Bunnage, M. E.; Harvey, J. W.; Mathias, J. P. A U.S. Patent Appl. Publ. US 2005020611, 2005.
34. Sokolov, Yu. A. *Vest. Natsyyanal. Akad. Belar.* **2000**, *2*, 76–80.
35. Huff, B. E.; Staszack, M. A. *Tetrahedron Lett.* **1993**, *34*, 8011–8014.
36. Bouissane, L.; El Kazzouli, S.; Léger, J. M.; Jarry, C.; Rakib, E. M.; Khouili, M.; Guillaumet, G. *Tetrahedron* **2005**, *61*, 8218–8225.
37. Dai, W. M.; Guo, D. S.; Sun, L. P. *Tetrahedron Lett.* **2001**, *42*, 5275–5278.
38. Penning, T. D.; Djuric, S. W.; Miyashiro, J. M.; Yu, S.; Snyder, J. P.; Spangler, D.; Anglin, C. P.; Fretland, D. J.;

Kachur, J. F.; Keith, R. H.; Tsai, B. S.; Villani-Price, D.; Walsh, R. E.; Widomski, D. L. *J. Med. Chem.* **1995**, *38*, 858–868.
39. Murphy, M. E.; Noack, E. *Methods Enzymol.* **1994**, *233*, 240–250.
40. Sekkai, D.; Guittet, O.; Lemaire, G.; Tenu, J. P.; Lepoivre, M. *Arch. Biochem. Biophys.* **1997**, *340*, 117–123.
41. Lepoivre, M.; Flaman, J. M.; Henry, Y. *J. Biol. Chem.* **1992**, *267*, 22994–23000.
42. Abu-Soud, H. M.; Gachhui, R.; Raushel, F. M.; Stuehr, D. J. *J. Biol. Chem.* **1997**, *272*, 17349–17353.
43. McMillan, K.; Masters, B. S. S. *Biochemistry* **1993**, *32*, 9875–9880.
44. Salerno, J. C.; Frey, C.; McMillan, K.; Williams, R. F.; Masters, B. S.; Griffith, O. W. *J. Biol. Chem.* **1995**, *270*, 27423–27428.
45. Klatt, P.; Schmid, M.; Leopold, E.; Schmidt, K.; Werner, E. R.; Mayer, B. *J. Biol. Chem.* **1994**, *269*, 13861–13866.
46. Mayer, B.; Klatt, P.; Werner, E. R.; Schmidt, K. *Neuropharmacology* **1994**, *33*, 1253–1259.
47. Matsuoka, A.; Stuehr, D. J.; Olson, J. S.; Clark, P.; Ikeda-Saito, M. *J. Biol. Chem.* **1994**, *269*, 20335–20339.
48. Abu-Soud, H. M.; Feldman, P. L.; Clark, P.; Stuehr, D. J. *J. Biol. Chem.* **1994**, *269*, 32318–32326.
49. Klatt, P.; Heinzel, B.; John, M.; Kastner, M.; Bohme, E.; Mayer, B. *J. Biol. Chem.* **1992**, *267*, 11374–11378.
50. Davies, R. R. *J. Chem. Soc.* **1955**, 2412–2423.
51. Moali, C.; Boucher, J. L.; Sari, M. A.; Stuehr, D. J.; Mansuy, D. *Biochemistry* **1998**, *37*, 10453–10460.
52. Wu, C.; Zhang, J.; Abu-Soud, H.; Ghosh, D. K.; Stuehr, D. J. *Biochem. Biophys. Res. Commun.* **1996**, *222*, 439–444.
53. Ghosh, S.; Gachhui, R.; Crooks, C.; Wu, C.; Lisanti, M. P.; Stuehr, D. J. *J. Biol. Chem.* **1998**, *273*, 22267–22271.
54. Bradford, M. M. *Anal. Biochem.* **1976**, *72*, 248–252.
55. Stuehr, D. J.; Ikeda-Saito, M. *J. Biol. Chem.* **1992**, *267*, 20547–20550.